ABSTRACT

MATAR, WALID OMAR. Integral Analysis of Turbulent Natural Convection with Condensation in the Presence of a Noncondensable Gas. (Under the direction of Dr. James Leach.)

An approximate model is presented for turbulent natural convection flow of a two-component mixture in which condensate forms along a vertical wall. The integral method is employed as the scheme for the analysis of the gas boundary layer. By incorporating empirical correlations and profiles for temperature, velocity, and density, the compressible Navier-Stokes equations are solved for boundary layer thickness and maximum velocity. Eventually, the desired physical characteristics of heat flux and condensation rate are determined. The major constraint enforced in the model is that the water within the boundary layer is either saturated vapor or slightly superheated. Local condensation away from the wall is not considered. A diverse range of mixtures were studied to examine the effects of noncondensable gas concentration on the heat transfer and condensation rates. It is shown in the results how the presence of air is a hindrance to the diffusion of vapor through the gas boundary layer. The results are compared to a previous empirical model. The results showed reasonable agreement with the previous experimental study discussed. For very large and often times more applicable temperature differences, the model predicts volumetric condensation within the gas boundary layer. A semi-empirical one-equation turbulence model was introduced, and although the turbulent impact on effective properties was determined to be small, it was included nonetheless for flexibility. Code logic and methodology are presented to automate this problem, as the solution is obtained through the iteration on both the turbulent viscosity and the interface temperature.

Integral Analysis of Turbulent Natural Convection with Condensation in the Presence of a Noncondensable Gas

by
Walid Omar Matar

A thesis submitted to the Graduate Faculty of
North Carolina State University
in partial fulfillment of the
requirements for the Degree of
Master of Science

Mechanical Engineering

Raleigh, North Carolina

2010

APPROVED BY:

_____	_____
Dr. James Leach Chair of Advisory Committee	Dr. Herbert Eckerlin Co-chair of Advisory Committee
_____	_____
Dr. Tiegang Fang	Dr. James Selgrade

BIOGRAPHY

Walid Matar was born in Yanbu, Saudi Arabia on August 11, 1986 to Omar Matar and Manal Esmail. After completing fifth grade in Jeddah, Saudi Arabia, he and his family moved to the United States. He graduated high school in 2004, and attended the University of South Carolina where he studied mechanical engineering. Upon graduating in 2008, he pursued higher education at North Carolina State University.

ACKNOWLEDGEMENTS

I want to thank my parents, Manal and Omar, for without them and their support, I would not have this opportunity. They have given so much to my siblings and I so that we can have the chance to excel. I want to also thank my siblings for their support. I was provided great guidance and support from my advisor, Dr. James Leach, throughout my study at North Carolina State University. I greatly appreciate his involvement and knowledge input. I am thankful for all the knowledge and education provided by the faculty and staff throughout my studies in the Department of Mechanical and Aerospace Engineering. Lastly, I want to thank Dr. Scott Ormiston of the University of Manitoba and Mr. Brett Mattingly for clarifying their published works through my correspondence with them. Their input has helped significantly in my understanding regardless if it were fully incorporated into this work.

TABLE OF CONTENTS

LIST OF TABLES

LIST OF FIGURES

NOMENCLATURE

c_p – Specific Heat $\left[\frac{J}{kg \cdot K}\right]$

D – Mass Diffusion Coefficient $\left[\frac{m^2}{sec}\right]$

g – Gravitational Acceleration $\left[\frac{m}{sec^2}\right]$

Gr – Grashof Number

h – Heat Transfer Coefficient $\left[\frac{W}{m^2 \cdot K}\right]$

H – Enthalpy $\left[\frac{J}{kg}\right]$

k – Thermal Conductivity $\left[\frac{W}{m \cdot K}\right]$

l – Mixing Length $[m]$

M – Molar Mass $\left[\frac{g}{mol}\right]$

$m'' -$ Mass Flux $\left[\frac{kg}{m^2 \cdot sec}\right]$

P – Pressure $[Pa]$

Pr – Prandtl Number

$q'' -$ Heat Flux $\left[\frac{W}{m^2}\right]$

R – Gas Constant $\left[\frac{J}{kg \cdot K}\right]$

R_u – Universal Gas Constant $\left[\frac{J}{kmol \cdot K}\right]$

Sc – Schmidt Number

Sh – Sherwood Number

T – Temperature $[K]$

TKE – Turbulent Kinetic Energy $\left[\frac{m^2}{sec^2}\right]$

u – Velocity in the x-Direction $\left[\frac{m}{sec}\right]$

v – Velocity in the y-Direction $\left[\frac{m}{sec}\right]$

X – Molar Fraction

Greek Symbols

α – Thermal Diffusivity $\left[\frac{m^2}{sec}\right]$

β – Thermal Expansion Coefficient $[K^{-1}]$

δ – Boundary Layer Thickness $[m]$

ρ – Mass Density $\left[\frac{kg}{m^3}\right]$

τ – Shear Stress $[Pa]$

μ – Dynamic Viscosity $\left[\frac{N \cdot sec}{m^2}\right]$

ν – Kinematic Viscosity $\left[\frac{m^2}{sec}\right]$

Subscripts and Superscripts

∞ – Free Stream

a – Air

avg – Average

cond – Condensation

conv – Convection

eff – Effective Quantity; Includes both turbulent and molecular property

f – Film

g – Gas Boundary Layer

i – Gas-Liquid Interface

v - Vapor

w – Wall

t – Turbulent

INTRODUCTION

A turbulent steady state free convection heat and mass transfer problem is analyzed where vapor condenses on a vertical isothermal wall. This type of problem is vital in design of safe nuclear containment systems, but it is applicable to more general design measures. In an accident involving a nuclear reactor vessel, containment systems are designed to contain the steam and radioactive material that escapes. A passive cooling process then ensues where condensate begins to form on the cooler containment wall, and as a result, pressure is reduced inside the structure. The postulated problem is one of several measures incorporated to ensure safety in the case of a nuclear reactor accident [1].

In this analysis, only the gas boundary layer is considered due to the large thermal resistance it imposes relative to the liquid film. The objective in this work is not only to solve the problem and obtain a good approximate mathematical model, but the model will also be programmed for automated computation. There are two major phenomena that dictate the heat transfer rate, natural convection and the condensation of the steam. Both are discussed in depth below.

A schematic of the problem at hand is illustrated in Figure 1. The partial pressure variation, and thus the density gradient, is indicative of the direction of mass diffusion of the vapor. The decrease of the vapor pressure as the wall is neared is fully compensated for by the increase in the partial pressure of the air; the total static pressure is postulated as constant. The partial pressure of the air outside the gas boundary layer is constant, and it is preset at one atmosphere for the analysis.

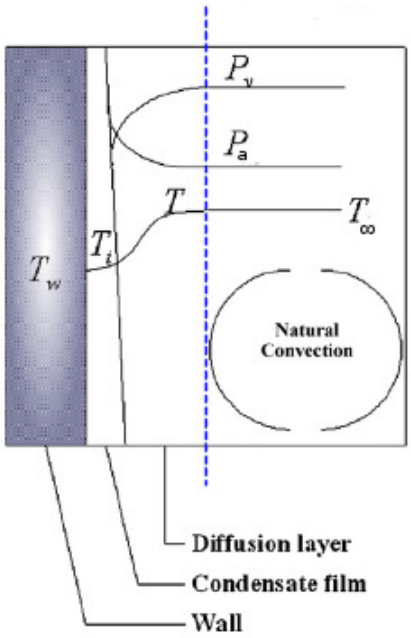

Figure 1 – Natural convection heat transfer system with condensation (Adapted from [2])

Natural Convection: Heat and Mass Transfer

Convection due to the temperature difference and the motion of the fluid contributes to the heat transfer to be analyzed. To elaborate, when a fluid is introduced into an environment in which a wall at a sufficiently lower temperature is present, the gravitational force induces a flow adjacent to the wall. The particles nearest to the wall will have a lower temperature than those farther from it. The variation in temperature that results is coupled with the fluid attaining larger density near the wall than away from it. The cooler particles begin to descend, while the warmer particles will rise. With the velocity increasing, a natural convection flow develops.

Eventually, in this case, a liquid film forms along the wall due to the vapor condensing, and a steady state boundary layer flow develops outside of it; two separate but

related flows result, as illustrated in Figure 1. One is comprised of water in liquid form, and one pertains to the air-vapor mixture flow. Furthermore, the gas-liquid interface that develops between the two boundary layers is characterized by the saturation temperature corresponding to the local vapor pressure. The largest thermal resistance is imposed by the gas boundary layer, and that is the reason its importance is emphasized. At the gas boundary layer edge, the partial pressures and temperature are at equilibrium.

For sufficiently tall vertical surfaces, turbulent flow typically results due to the increased intensity of flow with distance. The effect of turbulence on this aspect of analysis can be qualitatively predicted within reason. The instability results in larger heat transfer compared to laminar flow. Turbulence in natural convection takes place when the fluid travels at high velocity values; the critical distance at which the flow transitions from laminar to turbulence is commonly defined by a Grashof number of 10^9. Bejan and Lage showed that this is in fact the criterion of transition, improving upon previous established thought that suggested the criterion being a Rayleigh number of the order of 10^9 [3]. The local Grashof number, which is a ratio of the buoyant and viscous forces, is formulated below.

$$Gr_x = \frac{g\beta(T_\infty - T_i)x^3}{{\nu_{avg}}^2} \quad (1)$$

The instability that defines turbulent flow results in macroscopic eddies. The physical implication of the instability is the seemingly random fluctuations in the parameters associated with the flow. The intensity of the fluctuations may be large or small, and that will be determined for this case. The inclusion of turbulence modeling is heavily dependent by

the geometry associated with the flow, so the results to be presented are exclusive to the semi-infinite vertical wall layout.

Furthermore, due to the density gradient across the gas boundary layer, Fickian diffusion also affects the heat transfer in the overall system. The concentration of vapor is significantly smaller near the wall in comparison to the mixture near the boundary layer edge. This means the vapor diffuses toward the wall. The opposite holds true for the noncondensable gas. Because the gas-liquid interface is essentially impermeable to the noncondensable gas in the mixture, a great amount of air accumulates there. A viable model must consider these mass transfer mechanisms. The gases involved will be treated as ideal.

Condensation

Condensation is one of the key players in passive heat removal when an accident occurs in a nuclear containment vessel. The presence of the air is a hindrance to the condensation process. The accumulation of the air at the interface decreases the ability for the vapor to diffuse to the interface. The rate of condensation is heavily influenced by the amount of vapor that can diffuse toward the wall or is forced through by the buoyancy-induced motion.

The majority of the heat transfer in the analysis is expected to result from the condensation that occurs at the gas-liquid interface. In this work, a major constraint for the phase of the mixture is postulated; the vapor is assumed saturated or superheated throughout the gas boundary layer and free-stream regions. This means volumetric condensation within the boundary layer will not be introduced into the model. This is a significant assumption, and will play a role in the context of the results.

Moreover, one would think turbulence increases the rate of condensation, and thus the rate of heat release due to the phase transition. This is an important reason why more extensive examination and research are required for the system posed. The results obtained in this computation will be compared to existing experimental data for verification.

LITERATURE REVIEW

Turbulent Natural Convection

Due to the nature of the method employed to model this heat transfer process, obtaining justifiable approximation functions was among the first tasks to complete. The primary profiles to be determined were those of temperature and mean velocity in the vertical direction. Since the problem at hand involves turbulent natural convection along a vertical isothermal wall, the functions have to be representative of this type of flow. Initially, research focused on previous analyses and experiments conducted in flows where only air was present. It was felt that obtaining profiles from those problems would closely resemble the present problem.

The first journal article examined was that of Eckert et al published in 1951, where the integral method is used to solve a turbulent natural convection problem that involves air being heated near a vertical wall. Eckert's work included profiles for both temperature and vertical velocity. The temperature profile he published used the free-stream temperature as reference. Since the data was published so long ago, it was imperative that more research was conducted for verification. Eckert also used empirical correlations for heat transfer and shear stress at the wall that von Karman published several years earlier [4]. From the definition of shear stress and Fourier's Law, those two values can be related to velocity and temperature

gradients, respectively. The empirical correlations are important as they may be necessary in the semi-empirical analysis approach utilized in this work.

Textbooks and other published journal articles have questioned the temperature profile used by Eckert as given by Equation 2.

$$T = T_\infty + (T_w - T_\infty)\left[1 - \left(\frac{y}{\delta}\right)^{1/7}\right] \quad (2)$$

Warner, in 1967, published data that improves upon what Eckert et al reported. It was shown that the profile Eckert used in his work underestimated the temperature. The reason for the discrepancy between the two publications is given as instrumentation error. Warner asserts that the empirical formulation for temperature used by Eckert was obtained using inaccurate methods. The measurements were skewed due to conduction into the instrument's supports [5]. Warner's data was ultimately used to obtain a temperature profile for this analysis, as it was later corroborated by Cheesewright in 1982. Although Cheesewright did not present his data explicitly in that publication, he states that they are in good agreement with that of Warner.

In the same journal article, Cheesewright published data for the mean and fluctuation vertical velocity using Laser Doppler Anemometry. His data show that the mean velocity profile he obtained fell in line with what Eckert used in the 1950's; a comparison to show this is presented by Figure A-2 in Appendix A. The fluctuation velocity results are also important, as they can be ultimately related to the mean velocity and turbulent kinetic energy [6]. To summarize, the temperature profile used in the condensation problem presented was

that obtained from Warner's experimental data, and the velocity profile used was the same as the one Eckert used.

Integral Method Analysis

The integral method was first applied to free convection systems by Squire in 1938 [7]. The results obtained were very good, as documented by many publications. The problem studied at the time included a single noncondensable fluid and incompressible flow. Although he assumed that the dynamic and thermal boundary layers were the same, the heat transfer results proved viable for fluids that deviated away from that condition.

Turbulence Modeling

Because the problem consists of turbulent flow, many mathematical turbulence models were examined. The algebraic turbulence model finalized by Prandtl was studied first. It was determined that the model does not work in this problem, as it only works if the wall is impermeable. Since only the gas boundary layer is analyzed here, the so-called wall is not impermeable; condensate passes through the gas-liquid interface. The algebraic model always predicts a zero turbulent viscosity at the wall, and that cannot be the case here. The algebraic model would be best suited for analysis of the liquid film.

Examining alternative models, both one-equation and two-equation models incorporate turbulent kinetic energy, but two-equation models are much better to use as they incorporate a second parameter; this means a person does not have to make any rash assumptions. With one-equation modeling, an assumed mixing length expression would have to be introduced. Explicitly, these models would not be compatible with the method of solution to be carried out. Ultimately, and after more research, the turbulence intensity data

from Cheesewright's previously-discussed publication were found to be useful in this portion of the computation. The process of determining the turbulent flow properties will be discussed in a later section.

Experimental Studies

Furthermore, literature was also reviewed to be able to eventually compare results obtained by the model used in this problem to empirical correlations. The experimental work of Uchida and Tagami has been historically and frequently used in analyzing this problem. In 1965, they performed the same experiment while Tagami designed his own in presenting empirical formulations to model this problem. In the two experiments performed, the temperature of the wall was maintained at 49 ^{o}C. First, they both worked on an experiment in which a 30-cm-tall apparatus was used. Steam was steadily introduced to induce a pressure rise in the system, and the flow was allowed to equilibrate. Based on the mass ratio of the air and steam in the free-stream mixture, the following average heat transfer coefficient correlation was proposed.

$$\bar{h}_{Uchida} = 379\left(\frac{m_a}{m_v}\right)^{-0.707} \quad (3)$$

Tagami performed the same experiment himself in which a 90-cm-tall cylinder was utilized. Everything else in the design of the experiment remained constant to his previous work. His steady state correlation for the heat transfer coefficient is shown below. The initial noncondensable gas pressure was maintained at 1 atmosphere in both experiments [8].

$$\bar{h}_{Tagami} = 11.4 + 284\left(\frac{m_v}{m_a}\right) \quad (4)$$

The two above correlations are only valid when the wall temperature is 49 ^{o}C, and they do not seem to be in good agreement with one another for all cases. Also, in comparison to more recent models, the above correlations produce larger values for heat flux. Many thermodynamic properties and parameters were also not measured. These include the velocity of the flow and the pressure. More general and recent correlations must be examined.

In 1993, Peterson formulated experimental correlations for Nusselt and Sherwood numbers that would be the basis of his theoretical turbulent diffusion model for natural convection. Similar to the thermal conductivity relationship with Nusselt number, Peterson derived an expression for condensation thermal conductivity to relate it to the Sherwood number; it is given by Equation 5.

$$k_{cond} = \frac{1}{\phi T_{avg}} \left(\frac{{H_{fg}}^2 P_o {M_v}^2 D_o}{{R_u}^2 {T_o}^2} \right) \tag{5}$$

The conductivity is found at some reference temperature and pressure. ϕ is the gas-vapor log mean concentration ratio, given by,

$$\phi = -\frac{ln(P_{v,\infty}/P_{v,i})}{ln\left[\frac{1-P_{v,\infty}/P}{1-P_{v,i}/P}\right]} \tag{5a}$$

The conductivity also approaches zero as the free-stream mole fraction of the noncondensable gas increases. This is expected, as sensible convection would be the dominant heat transfer mechanism when there is very little steam. The Nusselt and Sherwood number relations Peterson recommends for natural convection with vertical flat surfaces are given by Equations 6 and 7, respectively [9]. These numbers are then used to determine heat

transfer coefficients, and ultimately the heat flux. The benefit of this model is that the correlations are not constrained to a specific wall temperature or free-stream air partial pressure conditions. The McAdams relation calls for coefficients of 0.13 to account for increased mist near the interface, but the coefficients of 0.1 are maintained as presented by Peterson [8].

$$Nu_x = 0.1(Gr_x Pr)^{1/3} \quad (6)$$

$$Sh_x = 0.1(Gr_x Sc)^{1/3} \quad (7)$$

For conservative design, Peterson recommends setting the ratio of the coefficients of the two dimensionless numbers as unity.

ANALYSIS PROCEDURE

The integral method is a popular approximation solution method with natural convection problems. This is due to the complex nature of solving the Navier-Stokes equations directly with such problems; this method will be employed in this analysis of steady-state two-dimensional flow. The integral analysis will be performed to obtain semi-empirical approximate algebraic solutions to the conservation equations. To utilize it, one must incorporate models and profiles from other similar analyses. It must be known that those models would approximately resemble the problem at hand. Historically, this type of analysis has generated reasonable results, and by comparing the results obtained in this problem to empirical data, the same will be shown here.

Firstly, a coordinate system is established on which the governing equations can be solved. The origin is set as the leading edge of the boundary layer. The *x*-axis represents the

vertical axis, and it is denoted as positive downward. The *y*-axis represents the horizontal axis, and it is positive in the direction away from the gas-liquid interface.

Since the gravity-induced natural convection flow is enforced by the temperature variation, and more importantly the density variation, the thermal and dynamic boundary layers will be approximated as equal in value; they are denoted by one parameter, δ_g. Vapor and air have Prandtl numbers that are close to unity. Although using a fluid that has a very high or very low Prandtl number theoretically alters this condition of equality, the work of Squire shows that his solution for heat transfer rate was still valid for fluids with a wide range of momentum and thermal diffusion properties.

The compressible two-dimensional conservation laws that must be satisfied are represented by Equations 8-10, below.

$$\frac{\partial}{\partial x}(m''_x) + \frac{\partial}{\partial y}\left(m''_y\right) = 0 \tag{8}$$

$$\frac{\partial}{\partial x}(\rho u^2) + \frac{\partial}{\partial y}(\rho uv) = -\frac{\partial P}{\partial x} + \frac{\partial}{\partial y}\left(\mu\frac{\partial u}{\partial y} - \overline{u'v'}\right) + g\rho \tag{9}$$

$$\frac{\partial}{\partial x}(\rho uH) + \frac{\partial}{\partial y}(\rho vH) = \frac{\partial}{\partial y}(k\frac{\partial T}{\partial y} - \rho c_p\overline{v'T'}) + \frac{\partial}{\partial y}\left(\mu u\frac{\partial u}{\partial y}\right) \tag{10}$$

To elaborate, Equation 8 represents the conservation of mass. Since the transient terms are neglected, the mass leaving the control volume must equal the mass entering. Equation 9 models the conservation of momentum in the vertical direction, and it is a representation of Newton's second law. The left side of the equation represents the fluid's inertia in the flow. The right side of the equation represents the effects of the pressure gradient, friction, and the body force acting on the fluid. The conservation of momentum in

the horizontal direction is neglected because the equation has minimal effect on the system; this can be shown by comparing the scale of the equations. Equation 10 represents the conservation of thermal energy. The left-hand side models heat transfer through convection, and the right-hand side models conduction and heat transfer from friction. Usually, the effect of friction is neglected. Especially in natural convection, friction has negligible impact on the heat transfer.

Specific heat for each component will be approximated as a constant value, rather than a function of temperature; the effect of the variation is minimal in this problem. The enthalpy in the energy equation will be modeled by Equation 10a. For convenience, the reference temperature used in the integration will be that of the free-stream mixture.

$$H = \int_{T_\infty}^{T} c_p dT \tag{10a}$$

The effect of turbulence on the system is noted by the inclusion of fluctuations in the flow; those fluctuation terms are denoted with an apostrophe in the above equations. They pertain to temperature and velocity. Physically, the fluctuations result from the instability of the flow. The fluctuations are mathematically related below by Equations 11 and 12. The mean of the product of the fluctuation values is negative, so the physical values for turbulent heat transfer and shear stress are written with a positive sign.

$$q''_t = -\rho c_p \overline{v'T'} = -k_t \frac{\partial T}{\partial y} \tag{11}$$

$$\tau_t = -\overline{u'v'} = \mu_t \frac{\partial u}{\partial y} \tag{12}$$

Using the fluid statics definition of pressure, the derivative of the pressure with respect to the horizontal direction is derived to be $-\rho_\infty g$. Substituting this, along with

Equations 11 and 12, results in the following *x*-momentum and energy equations. The sums of the viscosity and thermal conductivity values in the equations result in effective values for each respective property; they will be symbolized as such in subsequent discussion.

$$\frac{\partial}{\partial x}(\rho u^2) + \frac{\partial}{\partial y}(\rho uv) = \frac{\partial}{\partial y}\left[(\mu + \mu_t)\frac{\partial u}{\partial y}\right] + g(\rho - \rho_\infty) \tag{13}$$

$$\frac{\partial}{\partial x}(\rho uH) + \frac{\partial}{\partial y}(\rho vH) = \frac{\partial}{\partial y}\left[(k + k_t)\frac{\partial T}{\partial y}\right] \tag{14}$$

To solve the problem, approximate profiles for mean vertical velocity, temperature, and vapor density are substituted into the conservation equations. Then, they will be integrated, resulting in a simpler system of first-order ordinary differential equations. The system will be solved for gas boundary layer thickness, maximum velocity in the vertical direction, and a third parameter that will be imposed to assure mass is conserved. The approximate equations for velocity and temperature are given below in Equations 15 and 16, respectively.

$$u(x,y) = 1.862u_{max}\left(\frac{y}{\delta_g}\right)^{1/7}\left(1 - \frac{y}{\delta_g}\right)^4 \tag{15}$$

$$\theta(x,y) = \begin{cases} 1 - 5.59\left(\frac{y}{\delta_g}\right)^{2/3}, & 0 \le \frac{y}{\delta_g} \le 0.059 \\ 1.929\left[1 - \left(\frac{y}{\delta_g}\right)^{1/7}\right]^2, & 0.059 < \frac{y}{\delta_g} \le 1 \end{cases} \tag{16}$$

Temperature is normalized as,

$$\theta(x,y) = \frac{T(x,y) - T_\infty}{T_i - T_\infty} \tag{16a}$$

It was difficult to obtain a single equation that sufficiently and accurately fit Warner's data, so a two-equation path was chosen; it provided a much better fit. Commercial software

was used for assistance in the curve-fitting. Maple's least squares function was incorporated. In Appendix A, Equation 16 is compared to the data provided by Warner as well as the curve used by Eckert. The gas boundary layer thickness and the maximum vertical velocity are functions of the *x*-direction only.

In historical analyses of simpler and similar natural convection flows, the Boussinesq approximation has been usually incorporated. It states that the density is assumed constant throughout the conservation equations, with the exception of the buoyancy term; it must not be constant in the buoyancy term, or there would not be any buoyancy contribution modeled. This approximation will not be introduced here; the flow will be modeled as compressible in that regard. As noted previously, this model is to be solved for a condition in which the vapor is saturated throughout the boundary layer. Using this information, a vapor density profile can be obtained using the temperature equation. Many temperature conditions were used to find saturated vapor density across the boundary layer for each case. Eventually, a vapor density profile was fit. It is given by Equation 17, below. Like temperature, a piecewise function could have been used to represent the vapor density, but it was ultimately found that the difference was not significant in the grand scheme of the analysis.

$$\rho_v(x,y) = \rho_{v,\infty} + \left(\rho_{v,i} - \rho_{v,\infty}\right)\left[1 - \left(\frac{y}{\delta_g}\right)^{3/2}\right]^2 e^{A\frac{y}{\delta_g}} + \lambda\left(\frac{y}{\delta_g}\right)\left(1 - \frac{y}{\delta_g}\right)^2 \qquad (17)$$

The value of *A* is determined by Equation 17a. The expression was found through the curve-fitting process. Many interface and free stream temperature pairs were used to find a density profile, and in each case, the coefficient of the exponent varied. Ultimately an

equation was formulated to be able to find the coefficient. The expression for *A* has been tested numerous times and it works in every case run.

$$A = 17.87\left(\frac{\Delta T}{T_\infty}\right)^2 + 4.538\left(\frac{\Delta T}{T_\infty}\right) - 17.742 \tag{17a}$$

Where,

$$\Delta T = T_i - T_\infty$$

The viability of the vapor density equation is shown for an example case in Appendix A.

Unlike everywhere else in this analysis, the input of Equation 17a is in the units of $\frac{^\circ C}{^\circ C}$; this is done because using Kelvin would make the curve-fitting process more difficult. The right-most term in Equation 17 includes a third variable, λ, which is incorporated to ensure mass is conserved and to account for cases where the vapor is superheated. Aside from the fact the overall equation must be fit to calculated data, the λ-term was chosen based on some criteria. The value of the term must be zero at the boundaries, and the slope of the term must be zero on the boundary layer edge; the term chosen satisfies the requirements.

The total mixture pressure remains constant throughout the boundary layer. Using Dalton's law of partial pressures and the ideal gas law, the air density is formulated in Equation 18. The expression also includes the profiles used to approximate other properties for the system.

$$\rho_a(x,y) = \frac{P}{R_a T(x,y)} - \frac{R_v}{R_a}\rho_v(x,y) \tag{18}$$

After some algebraic manipulation, Dalton's law is also used to obtain an expression for total density; it is given by Equation 19.

$$\rho(x,y) = \rho_a(x,y) + \rho_v(x,y) \tag{19}$$

There are two mechanisms involved in the mass transport process in the system. Fickian diffusion due to the concentration gradient is important, and it is significantly affected by turbulence. The other mechanism is due to the buoyancy-induced motion; there is a velocity component, as well. For a component in a binary mixture consisting of species A and B, the absolute mass flux in the *y*-direction is then given by the following equation [10].

$$m''_{A,y} = \rho_A v - \rho D_{AB,eff} \frac{\partial}{\partial y}\left(\frac{\rho_A}{\rho}\right) \tag{20}$$

As mentioned previously, diffusion in the vertical direction is neglected. So the mass transfer in the vertical direction will pertain exclusively to the gravity-induced velocity, and there will not be a concentration gradient contribution. The relation given in Equation 20 will be useful in ultimately determining the velocity in the horizontal direction.

Conservation of Mass

The continuity equation presented by Equation 8 can be written individually for each component in the mixture. For air, it is given as

$$\frac{\partial}{\partial x}\left(m''_{a,x}\right) + \frac{\partial}{\partial y}\left(m''_{a,y}\right) = 0 \tag{21}$$

After integrating Equation 21 along the gas boundary layer region with respect to the horizontal direction, the following is obtained.

$$\int_0^{\delta_g} \frac{\partial}{\partial x}\left(m''_{a,x}\right)dy + \left(m''_{a,y}\right)_{\delta_g} - \left(m''_{a,y}\right)_i = 0 \tag{21a}$$

Similarly for vapor, the continuity equation is,

$$\frac{\partial}{\partial x}\left(m''_{v,x}\right) + \frac{\partial}{\partial y}\left(m''_{v,y}\right) = 0 \tag{22}$$

At the boundary layer edge, the density does not change, so the motion attributed to the concentration gradient is zero. It is also known that air does not penetrate the gas-liquid interface, as only water is transferred through it into the liquid film. From that information and Equation 21a, the *y*-component of the velocity can be represented in relation to the remaining mass flux term at that location.

$$v_\infty = \frac{-1}{\rho_{a,\infty}} \int_0^{\delta_g} \frac{\partial}{\partial x}\left(m''_{a,x}\right) dy \tag{23}$$

In conjunction with that formulation, the individual components' continuity equations can be used jointly to derive a single equation that only includes integration of the *x*-direction velocity terms. This allows the integration to exclude any contribution from Fickian diffusion. The combined equation is presented below in integral form.

$$\int_0^{\delta_g} \frac{\partial}{\partial x}\left(m''_{v,x}\right) dy - \frac{\rho_{v,\infty}}{\rho_{a,\infty}} \int_0^{\delta_g} \frac{\partial}{\partial x}\left(m''_{a,x}\right) dy = \left(m''_{v,y}\right)_i \tag{24}$$

The mass flux of the vapor at the interface in the right-hand side of the equation is the total mass flux at that location. The approximate functions presented previously will be substituted into Equation 24, and the terms will be integrated; a differential equation will result. To determine the vapor mass flux at the interface in the horizontal direction, an interface velocity must be expressed. In Equation 20, the mass flux of the air at that location can be set to zero. The *y*-component velocity at the interface can be computed as a result. An expression for the value is presented below.

$$v_i = \frac{\rho}{\rho_{a,i}} D_{av,eff} \frac{\partial}{\partial y}\left(\frac{\rho_a}{\rho}\right)\Big|_{y=0} \tag{25}$$

Differentiating the density fraction in Equation 25 is not possible in this turbulent flow due to the fact the derivative approaches infinity as the wall is approached. To mitigate this, the differentiation will be related to the vapor density and empirical correlations. Incorporating the ideal gas law and manipulating, the following relationship is established.

$$\frac{\partial}{\partial y}\left(\frac{\rho_a}{\rho}\right) = \left(\frac{\rho_v}{\rho}\right)^2 \frac{\partial}{\partial y}\left(\frac{\rho}{\rho_v}\right) \tag{25a}$$

Further manipulation using the ideal gas law and Dalton's law is performed, resulting in the following expression.

$$\frac{\partial}{\partial y}\left(\frac{\rho}{\rho_v}\right) = \frac{-P}{TR_a\rho_v}\left(\frac{1}{\rho_v}\frac{\partial \rho_v}{\partial y} + \frac{1}{T}\frac{\partial T}{\partial y}\right) \tag{25b}$$

Equation 25 can be rewritten and simplified to obtain the following form.

$$v_i = -D_{av,eff} \frac{P}{P_{a,i}}\left(\frac{\rho_{v,i}}{\rho_i}\right)\left(\frac{1}{\rho_v}\frac{\partial \rho_v}{\partial y} + \frac{1}{T}\frac{\partial T}{\partial y}\right)\Big|_{y=0} \tag{26}$$

Despite the fact the differentiation has been simplified, the derivative of the vapor density at the gas-liquid interface is still undefined. The same problem that existed earlier still persists. Rather than use Equation 17, the assumption of the saturated state of the vapor will be enforced using an empirical correlation; this means even if the steam is superheated, the pressure would not be much lower. The saturated vapor pressure can be determined using the Antoine equation, and the pressure can be related to density using the ideal gas law. The Antoine equation, for water, is given below [11].

$$P_v = (10^5)e^{11.724 - \frac{3841.196}{T(x,y) - 45.14}} \tag{27}$$

Moreover, the derivative of temperature in Equation 26 also poses the same problem as the density; another empirical correlation must be made. Eckert used an experimentally-derived expression for heat flux at the interface, as given by Equation 28, to bypass this issue. Using Fourier's law, the heat flux can then be directly related to the temperature gradient, as shown in Equation 29. This relation will be used throughout the analysis.

$$q''_w = 0.0359\rho c_p \Delta T {\nu_{eff}}^{1/4} {u_{max}}^{3/4} {\delta_g}^{-1/4} \tag{28}$$

Where,

$$\rho c_p = \rho_a c_{p,a} + \rho_v c_{p,v}$$

$$\left.\frac{\partial T}{\partial y}\right|_{y=0} = \frac{q''_w}{k_{eff}} \tag{29}$$

After some manipulation and incorporating the empirical relations, the local *y*-component velocity at the interface can be expressed by the below equation. Since the value is only valid at the interface, it is a function of the vertical direction only for a particular flow condition.

$$v_i = 0.0359 D_{av,eff} \frac{P {P'}_{v,i} \Delta T {\nu_{eff}}^{\frac{1}{4}} (\rho c_p)_i}{P_{a,i} R_v \rho_i k_{eff,i}} {u_{max}}^{3/4} {\delta_g}^{-1/4} \tag{30}$$

Where,

$$P'_{v,i} = \frac{3.841(10^8)}{T_i (T_i - 45.14)^2} e^{11.724 - \frac{3841.196}{T_i - 45.14}}$$

Conservation of Momentum

The inertia terms in the *x*-momentum equation can be integrated by substituting the velocity and density profiles. The *y*-component term is zero due to the vertical velocity

boundary conditions. At the interface, the no-slip boundary condition is enforced. At the boundary layer edge, the velocity is zero due to the disappearing influence of the density variation on the flow; the dynamic boundary layer edge is characterized by the zero velocity. Furthermore, the derivative of the vertical velocity in the viscous term approaches infinity as the interface is neared. Similar to the differentiation of temperature in the previous section, an empirical correlation to shear stress is made in this case. The correlation Eckert used for shear stress is expressed by Equation 31. It is related to the fluid mechanics definition of shear stress and directly used in the friction term.

$$\tau_w = \mu \frac{\partial u}{\partial y}\Big|_{y=0} = 0.0668 \rho {\nu_{eff}}^{1/4} {u_{max}}^{7/4} {\delta_g}^{-1/4} \quad (31)$$

When evaluating the viscous term, the value at the boundary layer edge is neglected since the velocity is zero. Equation 31 is only valid at the lower limit of the integration.

Conservation of Energy

In this steady state flow, the amount of heat being conducted through the so-called wall is the same amount of heat transferred through convection. For convection, both the vertical and horizontal components are incorporated. In the vertical direction, the difference of temperature may be small, but the velocity is large. The opposite situation is found in the horizontal component. It was decided that neither component would be neglected.

The heat flux expression given by Equation 28 is substituted into the conduction term for integration. Like the viscous term in the momentum equation, the heat flux is only valid at the interface. The change in temperature at the boundary layer edge is zero, thus the heat flux is zero.

To integrate all the terms in the conservation equations, a variable transformation is required. Rather than integrate with respect to *y*, the integrations are to be solved using the non-dimensional length of $\frac{y}{\delta_g}$. This coordinate results in a range of zero to unity, and greatly simplifies the integration.

Further steps have to be taken to solve the integrals. These steps do not apply to the code used to automate the solution of this problem. They only apply to the establishment of approximate algebraic equations. When integrating terms that involve a general density profile, an analytical solution is not achievable. For a specific wall and free-stream temperature condition, an analytical solution can be found. The problem arises when a general solution has to be obtained to represent any temperature pair imposition. Many values of $A\left(\frac{\Delta T}{T_\infty}\right)$ are used, and the resulting integration data set is curve-fit to obtain an algebraic equation. A similar process is adopted to solve the terms in the integration that include temperature in the denominator. It can be shown that the effect of these steps is minimal by comparing it to the code's output.

Turbulence Modeling

All the effective properties denoted in aforementioned equations include a molecular component and a turbulent component. Turbulence modeling is utilized to determine the latter components in the solution. A semi-empirical approach, combined with the one-equation model, was ultimately chosen to represent the instability in this flow. This will provide an idea of how significant the impact of turbulence is on this problem, and will eventually yield values for turbulent viscosity, mass diffusivity, and thermal conductivity.

The viscosity will be determined initially, and the latter two flow properties will be computed using turbulent Prandtl number and Schmidt number formulations. The turbulent kinetic energy, or TKE, can be modeled using the fluctuation velocity components. Since this is a two-dimensional problem, it is given as,

$$TKE = \frac{1}{2}\left(\overline{u'u'} + \overline{v'v'}\right) \tag{32}$$

Furthermore, due to the imposition of no-slip boundary conditions for the mean velocity in the vertical direction, exactly at the gas-liquid interface, the fluctuation in that direction is zero. Since there is permeability in that condensate crosses the boundary of the control volume, the velocity in the horizontal direction is not zero, as determined previously.

The viscosity model to be implemented is a one-equation model, given by Equation 33; C_μ is an empirical constant [12]. With one equation models, a mixing length must be known or estimated, as only the kinetic energy can be computed. On the interface, a mixing length approximation is expressed in terms of the boundary layer thickness by Equation 34.

$$\nu_t = C_\mu l (TKE)^{1/2} \tag{33}$$

Where,

$$C_\mu = 0.548$$

$$l = 0.09\delta_g \tag{34}$$

Using Cheesewright's aforementioned data for turbulence intensity, the fluctuation and mean velocity in the *x*-direction very close to the interface can be related by the equation below. It states that the maximum fluctuation velocity is roughly equal to 25% of the mean velocity at that location [4].

$$\frac{(\overline{u'u'})^{1/2}}{u} = 0.25 \tag{35}$$

It is hypothesized that since the fluctuation intensity is measured as 25% of the mean velocity in the vertical direction, the same intensity should apply for the flow in the *y*-direction at that same location. Employing this, the mean of the product of the fluctuation velocity in the horizontal direction is expressed as follows.

$$\overline{v'v'} = 0.0625{v_i}^2 \tag{36}$$

Finally, an equation for the turbulent kinematic viscosity at the interface is established in relation to the horizontal velocity, as shown by Equation 37. It is a function of the vertical direction only, since the expression is only valid at the gas-liquid interface, or when $y = 0$.

$$\nu_{t,i} = 0.176 C_\mu l v_i \tag{37}$$

The implicit expression above cannot be directly used in the onset to determine the viscosity, as the equation is coupled with other facets of the analysis. Initially, a guess is made, and an iterative process ensues from then on until the value converges. To determine the turbulent properties of mass diffusion coefficient and thermal conductivity, the following relationships are incorporated.

$$Pr_t = \frac{\nu_t}{\alpha_t} \tag{38a}$$

$$Sc_t = \frac{\nu_t}{{D_{a,v}}^t} \tag{38b}$$

Values for the molecular forms of the dimensionless numbers can be obtained using fluid properties to be discussed in a subsequent section. Equations 39a and 39b below relate the molecular quantities to their turbulent flow counterparts [13].

$$Pr_t = 0.85 + \frac{C_t}{Pr} \tag{39a}$$

$$Sc_t = 0.85 + \frac{C_t}{Sc} \tag{39b}$$

C_t is an experimentally-determined constant whose value is dependent upon the speed of the flow; it will be set at 0.01.

Other Mixture Properties

Determining the following air-vapor mixture properties is crucial in obtaining good results. The dynamic viscosity for air and saturated vapor is tabulated in many publications. The mixture dynamic viscosity is dependent upon the molar composition of the two components, and it is formulated by Equation 40 [14]. The mixture kinematic viscosity can be found by dividing the dynamic viscosity by total density.

$$\mu = \sum w_m \mu_m \tag{40}$$

Where,

μ_m = Dynamic viscosity of component *m*.

The weighting factor for component *m*, w_m, is given by,

$$w_m = \frac{X_m}{\sum_j a_{m,j} X_j} \tag{40a}$$

Where *a* is defined by,

$$a_{m,j} = \frac{\left[1+\left(\frac{\mu_m}{\mu_j}\right)^{0.5}\left(\frac{M_j}{M_m}\right)^{0.25}\right]^2}{\left[8\left(1+\frac{M_m}{M_j}\right)\right]^{0.5}} \quad (40b)$$

Using the viscosity, the thermal conductivity can be similarly determined using the empirical correlation presented by Equation 41; it is known as the Wassiljewa equation. Thermal conductivity for each component is also tabulated in various publications.

$$k = \sum d_m k_m \quad (41)$$

Where,

k_m = Thermal conductivity of component *m*.

For the *m*-th component, *d* is defined by,

$$d_m = \frac{X_m}{\sum_j b_{m,j} X_j} \quad (41a)$$

Where *b* is defined by,

$$b_{m,j} = 0.25\left(1 + \left[\frac{\mu_m}{\mu_j}\left(\frac{M_j}{M_m}\right)^{0.75}\frac{T+S_m}{T+S_j}\right]^{0.5}\right)^2 \frac{T+S_{m,j}}{T+S_m} \quad (41b)$$

Where,

$$S_{m\ (or\ j)} = 1.5T_{boiling}$$

$$S_{m,j} = \left(S_m S_j\right)^{0.5}$$

S is defined as the Sutherland constant, and it is dependent on the boiling point of the substance in question. For air, the value used for *S* is 110 K. An example showing how the mixture thermal conductivity is found is shown in Appendix B.

As stated previously, the transfer analyzed is not exclusive to heat; it also includes mass transfer. Due to its prevalence in many real world events, binary diffusion of water in air has seen extensive studies over the years. An empirical formula for the diffusion coefficient of vapor into air, and vice versa, is given by Equation 42. The correlation is valid in a temperature range of 280 K to 450 K [15]. Unlike elsewhere in the analysis, the pressure units used in the equation are atmospheres.

$$D_{av} = 1.87 \times 10^{-10} \frac{T^{2.072}}{P_{atm}} \tag{42}$$

Gas Boundary Layer Thickness and Maximum Velocity

To determine the boundary layer thickness and the maximum vertical velocity, the following general models are introduced.

$$\delta_g(x) = C_\delta x^n \tag{43}$$

$$u_{max}(x) = C_u x^m \tag{44}$$

The constants and power parameters are computed by solving the system of differential equations. They will be presented in a later section. Once these values and λ are found, the physical characteristics of most importance can be computed. These characteristics are total heat transfer from convection and condensation, and the rate at which vapor condenses at the interface.

The resulting solutions and assertions from performing this analysis only apply beyond the critical distance. Prior to that, the flow is modeled as laminar, and previous analyses have been completed with such flow considered.

The Interface Temperature

The only known temperature properties are those of the wall and the free stream mixture. The interface temperature is an unknown value in this problem. It is the saturation temperature, and it is computed by performing an energy balance on the gas-liquid interface. The energy balance takes into account the liquid film, the condensation, and the convection associated with the gas boundary layer; it is given below by Equation 45. After some manipulation, it can be written for the interface temperature, as shown in Equation 45a.

$$h_f(T_i - T_w) = (h_{cond} + h_{conv})(T_\infty - T_i) \tag{45}$$

$$T_i = \frac{h_f T_w + (h_{cond} + h_{conv}) T_\infty}{h_f + h_{cond} + h_{conv}} \tag{45a}$$

Many of the properties used to solve for the interface temperature in Equation 45a are actually dependent on it for computation. Due to this coupled aspect of the solution, an initial temperature value must be guessed in the onset of the analysis; an arithmetic mean between the free-stream and wall temperature values is computed for this. An iterative process eventually yields to a converged value, and that will be based on a predetermined convergence criterion of 0.0001 K.

To define the condensation and convection heat transfer coefficients, the resulting heat flux expressions associated with each mechanism are divided by the temperature difference across the gas boundary layer. In order to obtain an energy balance, a boundary layer thickness for the liquid film has to be known, as well. The heat transfer coefficient of the liquid film is defined by the ratio of the thermal conductivity to the film thickness. It is going to be assumed that the liquid film is laminar, and the film thickness incorporated is

introduced by Equation 46 [2]. This film thickness is documented in previous analyses dealing with condensing heat transfer in natural convection flow.

$$\delta_f = \left[\frac{4k_f\mu_f(T_i - T_w)}{g\rho_f(\rho_f - \rho_v)H'_{fg}}\right]^{1/4} x^{1/4} \quad (46)$$

The vapor density is much smaller than the density of water in liquid form, so the vapor density can be neglected in that equation. H'_{fg} is the corrected enthalpy of vaporization for the liquid film; it is given by Equation 47. The value is dependent on temperature. The enthalpy of condensation, which is significant in this problem, is the additive inverse of it. The corrected enthalpy of condensation used for the gas boundary layer is given by Equation 48. The enthalpy of condensation is a component of the heat transfer coefficient associated with the condensation.

$$H'_{fg} = H_{fg} + 0.68c_{p,f}(T_i - T_w) \quad (47)$$

$$H'_{gf} = H_{gf} + 0.68c_{p,v}(T_i - T_\infty) \quad (48)$$

RESULTS AND DISCUSSION

As a result of the integrations performed, three coupled non-linear ordinary differential equations are obtained. The approximate differential equation representing continuity is given below. Equations 50 and 51 represent momentum and energy, respectively.

Conservation of Mass

$$\frac{d}{dx}\left(\delta_g u_{max}\right)\left[\left(1 + \frac{P_{v,\infty}}{P_{a,\infty}}\right)\left(0.2726\rho_{v,\infty} + 0.0261\lambda + \Delta\rho_v A_1\right) - \frac{1.862PP_{v,\infty}}{T_\infty R_v P_{a,\infty}}(T_1)\right] = \rho_i v_i \quad (49)$$

Where,

$$A_1 = 2.5905(10^{-4})A^2 + 0.01093A + 0.16256$$

$$T_1 = 0.14643 - 0.02406\left(\frac{\Delta T}{T_\infty}\right) + 0.01516\left(\frac{\Delta T}{T_\infty}\right)^2$$

$$\Delta\rho_v = \rho_{v,i} - \rho_{v,\infty}$$

Conservation of Momentum

$$\frac{d}{dx}\left(\delta_g {u_{max}}^2\right)\left[\frac{3.467P}{R_a T_\infty}(T_2) + \left(1 - \frac{R_v}{R_a}\right)(0.1814\rho_{v,\infty} + 0.0147\lambda + \Delta\rho_v A_2)\right] =$$

$$\delta_g g\left[\left(1 - \frac{R_v}{R_a}\right)\left(\rho_{v,\infty} + 0.0833\lambda + \Delta\rho_v A_3\right) - \rho_\infty + \frac{P}{R_a T_\infty}(T_3)\right] + 0.0668\left[\left(\frac{R_v}{R_a} - 1\right)\rho_{v,i} - \frac{P}{R_a T_i}\right]{\nu_{eff}}^{1/4}{u_{max}}^{7/4}{\delta_g}^{-1/4} \quad (50)$$

Where,

$$T_2 = 7.3753(10^{-3})\left(\frac{\Delta T}{T_\infty}\right)^2 - 0.01104\left(\frac{\Delta T}{T_\infty}\right) + 0.05236$$

$$T_3 = 3.1692(10^{-2})\left(\frac{\Delta T}{T_\infty}\right)^2 - 0.05979\left(\frac{\Delta T}{T_\infty}\right) + 1.00015$$

$$A_2 = 8.4405(10^{-6})A^3 + 4.97(10^{-4})A^2 + 1.1922(10^{-2})A + 0.14794$$

$$A_3 = 3.1805(10^{-5})A^3 + 1.6398(10^{-3})A^2 + 3.1586(10^{-2})A + 0.276$$

Conservation of Energy

$$\frac{d}{dx}\left(\delta_g u_{max}\right)1.862\Delta T\left[\frac{c_{p,a}P}{R_a T_\infty}T_4 + c_{p,d}(0.0254\rho_{v,\infty} + 1.371(10^{-3})\lambda + \Delta\rho_v A_4)\right] =$$

$$\left[1 + D_{eff,i}\frac{\Delta TPP_{v,i}{}'}{\rho_i P_{a,i} R_v k_{eff,i}}\left(\frac{c_{p,a}P}{R_a T_i} + c_{p,d}\rho_{v,i}\right)\right]0.0359\Delta T{u_{max}}^{3/4}{\delta_g}^{-1/4}{\nu_{eff}}^{1/4}\left(\frac{c_{p,a}P}{R_a T_i} + c_{p,d}\rho_{v,i}\right) \quad (51)$$

Where,

$$c_{p,d} = c_{p,v} - \frac{R_v}{R_a} c_{p,a}$$

$$T_4 = 0.02546 - 8.3496(10^{-3}) \left(\frac{\Delta T}{T_\infty}\right) + 0.01041 \left(\frac{\Delta T}{T_\infty}\right)^2$$

$$A_4 = 0.0215 + 8.724(10^{-4})A + 1.678(10^{-5})A^2$$

The coefficients of each term in the *A* and *T* expressions are curve-fitting constants. To simplify the presentation of future equations, the following definitions are made. They denote coefficient values from the differential equation system.

$$Ta \equiv \left(1 + \frac{P_{v,\infty}}{P_{a,\infty}}\right)\left(0.2726\rho_{v,\infty} + 0.0261\lambda + \Delta\rho_v A_1\right) - \frac{1.862PP_{v,\infty}}{T_\infty R_v P_{a,\infty}}(T_1)$$

$$Ba \equiv 0.0359 D_{av,eff} \frac{PP'_{v,i}\Delta T \nu_{eff}^{\frac{1}{4}} (\rho c_p)_i}{P_{a,i} R_v k_{eff,i}}$$

$$B \equiv \frac{3.467P}{R_a T_\infty}(T_2) + \left(1 - \frac{R_v}{R_a}\right)(0.1814\rho_{v,\infty} + 0.0147\lambda + \Delta\rho_v A_2)$$

$$g' \equiv g\left[\left(1 - \frac{R_v}{R_a}\right)\left(\rho_{v,\infty} + 0.0833\lambda + \Delta\rho_v A_3\right) - \rho_\infty + \frac{P}{R_a T_\infty}(T_3)\right]$$

$$R \equiv 0.0668\left[\left(\frac{R_v}{R_a} - 1\right)\rho_{v,i} - \frac{P}{R_a T_i}\right]{\nu_{eff}}^{1/4}$$

$$F \equiv 1.862\Delta T\left[\frac{c_{p,a}P}{R_a T_\infty} T_4 + c_{p,d}(0.0254\rho_{v,\infty} + 1.371(10^{-3})\lambda + \Delta\rho_v A_4)\right]$$

$$\gamma \equiv \left[1 + D_{eff,i} \frac{\Delta T P P_{v,i}'}{\rho_i P_{a,i} R_v k_{eff,i}} \left(\frac{c_{p,a}P}{R_a T_i} + c_{p,d}\rho_{v,i}\right)\right] 0.0359\Delta T {\nu_{eff}}^{1/4} \left(\frac{c_{p,a}P}{R_a T_i} + c_{p,d}\rho_{v,i}\right)$$

Gas Boundary Layer Thickness and Maximum Velocity

After substituting Equations 43 and 44 into the approximate energy and *x*-momentum equations and solving simultaneously, *n* and *m* are determined to be 0.7 and 0.5, respectively.

Once these values are found, the general models were substituted into the same conservation equations again (The dependence on the distance is hence removed). This time, and after differentiation and algebraic manipulation, the constants C_δ and C_u were found; they are given by Equations 52 and 53, respectively.

$$C_\delta = \left(\frac{5\gamma}{6F}\right)^{4/5}\left(\frac{17B}{10g\prime} - \frac{6RF}{5\gamma g'}\right)^{1/10} \tag{52}$$

$$C_u = \left(\frac{17B}{10g\prime} - \frac{6RF}{5\gamma g'}\right)^{-1/2} \tag{53}$$

The third and final parameter needed to be able to solve this problem is λ. It is determined by incorporating the remaining conservation equation of the system, and it is that for mass; it is given by Equation 54. λ is computed before the other two unknown parameters.

$$\lambda = \frac{(Ba)(Tha)-(Alf)(\gamma)}{(\gamma)(c_1)-(Ba)(c_2)} \tag{54}$$

Where,

$$Tha = 1.862\Delta T\left[\frac{c_{p,a}P}{R_a T_\infty}T_4 + c_{p,d}(0.0254\rho_{v,\infty} + \Delta\rho_v A_4)\right]$$

$$Alf = \left(1 + \frac{P_{v,\infty}}{P_{a,\infty}}\right)\left(0.2726\rho_{v,\infty} + \Delta\rho_v A_1\right) - \frac{1.862PP_{v,\infty}}{T_\infty R_v P_{a,\infty}}(T_1)$$

$$c_1 = 0.0261\left(1 + \frac{P_{v,\infty}}{P_{a,\infty}}\right)$$

$$c_2 = 0.0255\Delta T c_{p,d}$$

Now that they are determined, the boundary layer thickness, the maximum velocity, and the λ values can be used to solve for the actual interface temperature value. Once the

temperature value converges, they can be substituted into the semi-empirical formulations for heat flux and condensation mass flux.

When solving this problem for specific cases, it became apparent that the interface velocity in the horizontal direction was extremely small. This means the kinetic energy for turbulence was also extremely small. This is a significant finding, and it means that turbulence has little impact on the flow at that location. Even with this in mind, the turbulent properties were still considered despite their small impact on the effective fluid properties. The small variation in the effective properties can still have a significant impact on the overall scheme for certain cases. It is also important to show the steps taken to model turbulence in the analysis.

The vital physical characteristics of condensation rate and heat transfer rate can now be determined. The local condensation mass flux, given by Equation 55, is simply the product of total density and the *y*-component velocity at the interface. The mass flux is actually negative, signaling a movement toward the wall given how the problem was set up. The negative sign was removed, however, by the inclusion of a positive temperature change in the equation.

$$m''_{cond} = 0.0359 D_{av,eff} \frac{PP'_{v,i}|\Delta T| {\nu_{eff}}^{\frac{1}{4}} (\rho c_p)_i}{P_{a,i} R_v k_{eff,i}} {u_{max}}^{3/4} {\delta_g}^{-1/4} \quad (55)$$

The heat flux at the interface is comprised of two components. The first component relates to convection, and the other is due to the condensation. The former is directly approximated through the empirical formulation Eckert used. The condensation heat release is found by multiplying the condensation mass flux, or the mass flux at the interface, by the

corrected enthalpy of condensation. The heat flux is given below; it is also negative, since energy is being released. As expected, the heat release due to the condensation is overwhelmingly larger than that through convection.

$$q''_{tot,i} = m''_{cond} H'_{gf} + q''_{conv} \quad (56)$$

Abiding by the local heat flux and shear stress formulations presented by von Karman, as the distance away from the leading edge increases, so do the heat flux and condensation mass flux values. Since this problem was analyzed with the mathematical emphasis of saturated vapor in the gas boundary layer, it is heavily not recommended to use these equations if there is volumetric condensation away from the interface.

Program

The code used to automate this problem was written in FORTRAN77. The general logic path of the code is illustrated in Figure 2. There are three required inputs; the free-stream temperature, the temperature of the impermeable wall, and a distance down the gas-liquid interface at which the solution will be calculated. Everything else, including physical constants, initial guesses, and conversions, is automatically performed as the program is executed.

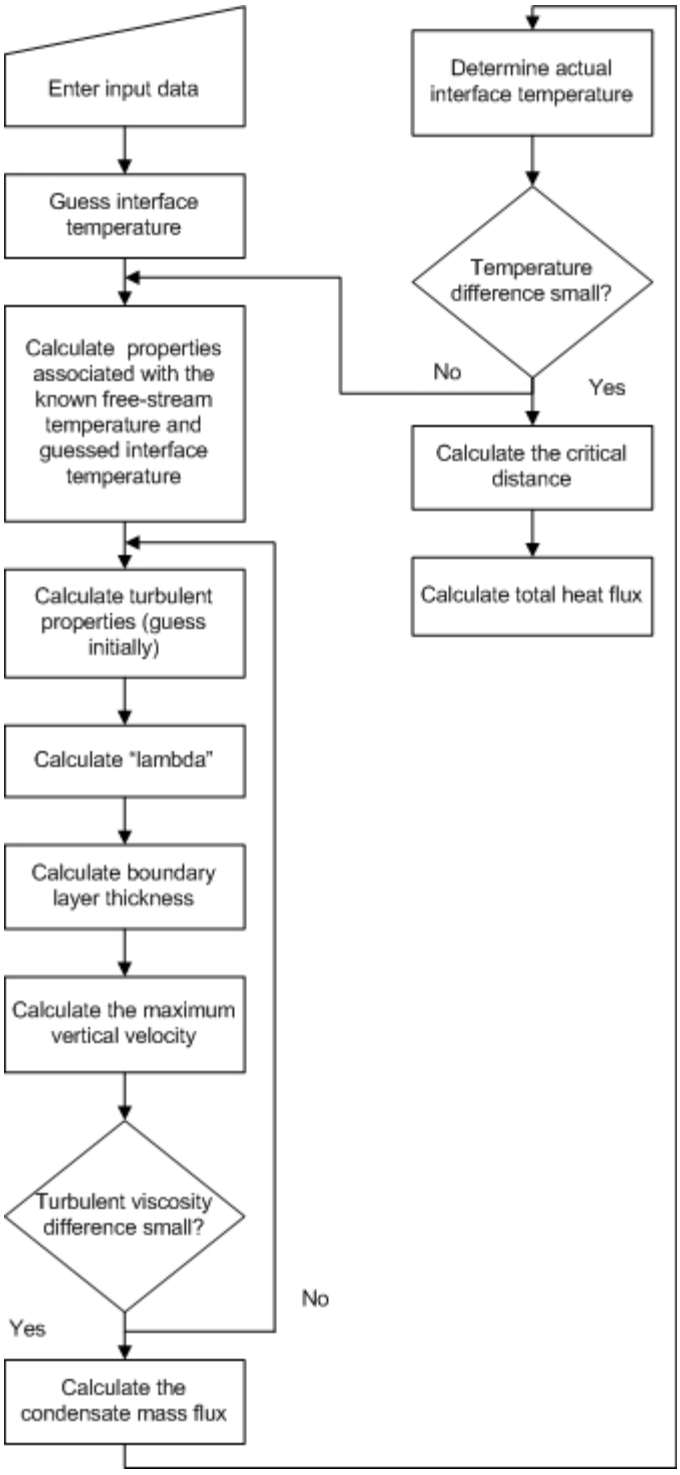

Figure 2 – Program flow chart

Theoretically, there are two large encompassing loops. The Newton-Raphson method is incorporated to iterate on the actual turbulent viscosity value. Numerical differentiation is adopted to perform this method. The step size for the differentiation has to be very small due to the naturally small order of magnitude of the viscosity value; in the program, the step size used is 10^{-8}. The step size cannot be too small, however, as round-off error may become a factor. After a run, the zero of the implicit turbulent viscosity function will be determined. If it converges, the computation proceeds to subsequent steps. The predetermined convergence criterion for turbulent viscosity is set at 10^{-9} m^2/sec.

Although turbulent flow properties are small relative to the molecular properties, the code can still account for them for flexibility. They can easily be neglected from the code if desired. The extra iterative procedure does require more processing time. The code associated with the turbulent viscosity convergence is presented in Appendix C.

The program does not utilize the approximate algebraic equations. The actual integrations are performed; practically, this is beneficial in that the results obtained using the algebraic equations can be easily compared to ensure their validity and accuracy. To perform the integration in the program, a fifth-order Newton-Côtes method was ultimately chosen. The major benefit in using Gaussian quadrature instead would be to have non-uniform intervals for the discretization of the area under the curve. Such feature is not necessary for this case. A general composite form of the Newton-Côtes formula was derived. The code associated with the integration is given in Appendix C.

The output of the program includes the local condensation mass flux, the local heat flux, the converged-upon interface temperature, the local gas boundary layer thickness, and

the local maximum velocity. Also, the heat flux is presented in separate components for condensation and convection. The code associated with the interface temperature is also shown in Appendix C. An interface temperature is calculated using the energy balance, and if the difference between the new value and the old value is sufficiently small, the program proceeds. If not, the new value becomes the new guess, and the program runs again using that updated value. The tolerance value for the temperature is preset at 0.0001 K.

Numerical Results and Data Comparison

The results of the program and approximate equations are to be presented and compared below. All the data to be presented are of a system in which the vapor is approximated to be saturated. To determine if the mixture quality is truly saturated in the gas boundary layer, the resulting vapor density profile for any given input data is compared to saturated values found in steam tables. There will be some discrepancy because the ideal gas model is incorporated in this analysis, but it is not significant.

Seven cases are chosen based on the ratio of the mass of noncondensable gas to that of the vapor in the free-stream region; it is desired to have a diverse range of free-stream conditions presented to see a relationship between the composition of the mixture and the heat transfer rate. This ratio is dictated by the temperature inputs at the wall and in the free-stream region. The first case is one where there is much more air than steam; specifically, the mass ratio is 10.86. A case that involves a mass ratio of around unity is also incorporated. The last case studied is one where there is much more vapor in the bulk region than air. The results and inputs associated with each case are presented below in Table 1. The interface temperature converged upon through the iteration is also shown.

Table 1 – Computed values for various free-stream mass ratio conditions

Wall Temperature (^oC)	Free-Stream Temperature (^oC)	Interface Temperature (^oC)	Free-Stream Mass Ratio (m_a/m_v)	Critical Distance (m)	Solution Distance (m)	Total Heat Transfer Coefficient (W/m^2K)
49	54	> 49	10.86	1.16	1.25	17.23
58	64	58.01	6.81	1.08	1.25	28.61
75	83	75.03	3.05	0.92	1.25	72.89
100	113	100.28	1.03	0.62	1.25	241.22
133	150	134.55	0.34	0.39	1.25	747.29
148	168	150.80	0.22	0.31	1.25	1049.14
175	201	181.22	0.1	0.21	1.25	1649.07

The interface temperature upon which the code converges is much closer to that of the wall, as should be expected. The difference between the wall and interface temperatures also increases with a more intense turbulent flow; i.e. larger temperature difference. To maintain uniformity in comparison, all the results were computed at a distance of 1.25 meters down the wall. The critical distance of the first case is so large, that for some containment vessels experiencing such conditions, the entire flow may be laminar. The results tabulated are only applicable beyond the critical distance.

Because the energy balance at the interface is performed between a laminar liquid film and a turbulent mixture in the gas boundary layer, there is no way to remove the interface temperature's dependence on distance. As the distance down the wall increases, the calculated interface temperature slightly increases, as well. The walls of containment vessels are not usually very long, so this does not pose a problem for those cases. Also, at distances far away from the leading edge of the flow, one would expect the liquid film to become unstable, as well.

It is observed that in forcing saturation quality on the boundary layer mixture, the difference in temperature required to abide by such postulation would have to be relatively small. In many applications, including passive cooling in a nuclear containment vessel, the temperature difference is much larger. In order to have saturated vapor at 54 ^{o}C for a wall at 49 ^{o}C, for example, the saturation pressure in the bulk region must be very low; there can certainly be applications in which that is the case, but it is unusual. The saturated vapor requirement of the analyses is a constraint on the change in temperature values. As the temperature difference is increased from the value that satisfies this requirement, the results show the vapor density is larger than the value associated with the saturated state. In reality, many applications have large temperature changes, and as such, this model predicts that there would be vapor condensing within the boundary layer for those cases. This mist formation would augment the heat transfer rate. It is not recommended to use this model to solve problems in which the density of the vapor exceeds the value associated with the saturation condition anywhere in the control volume.

The condensation mass flux and the heat flux at the interface obtained from the proposed model are plotted below for those aforementioned cases. Figures 3 and 4 show the values plotted against the mass ratio in the free-stream region.

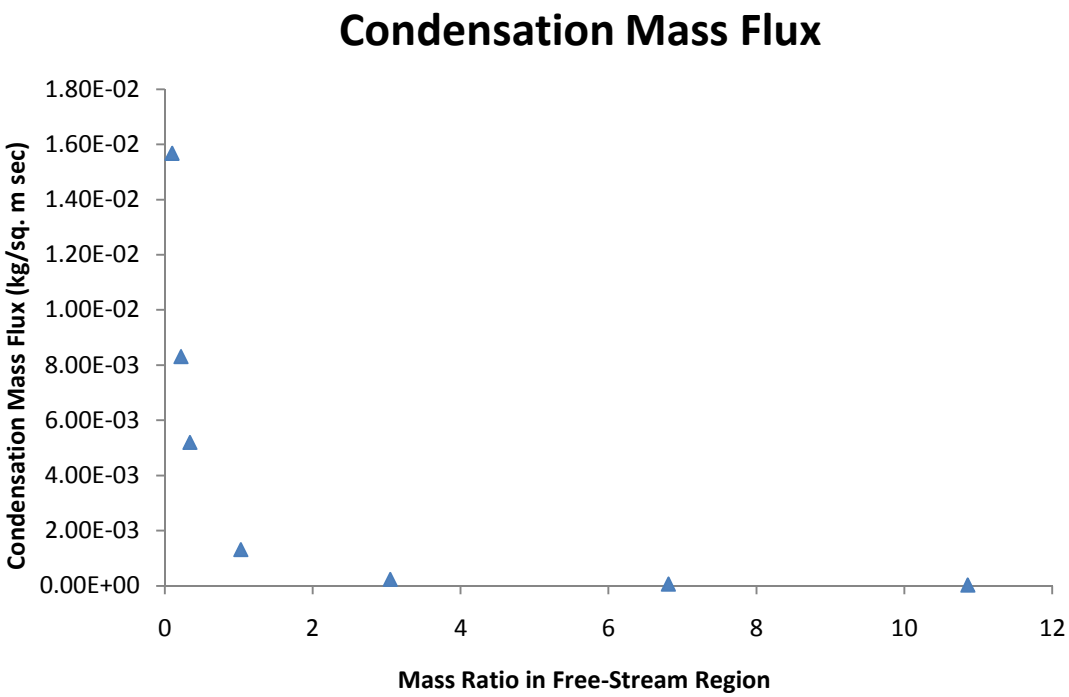

Figure 3 – Condensation mass flux with changing free-stream temperature

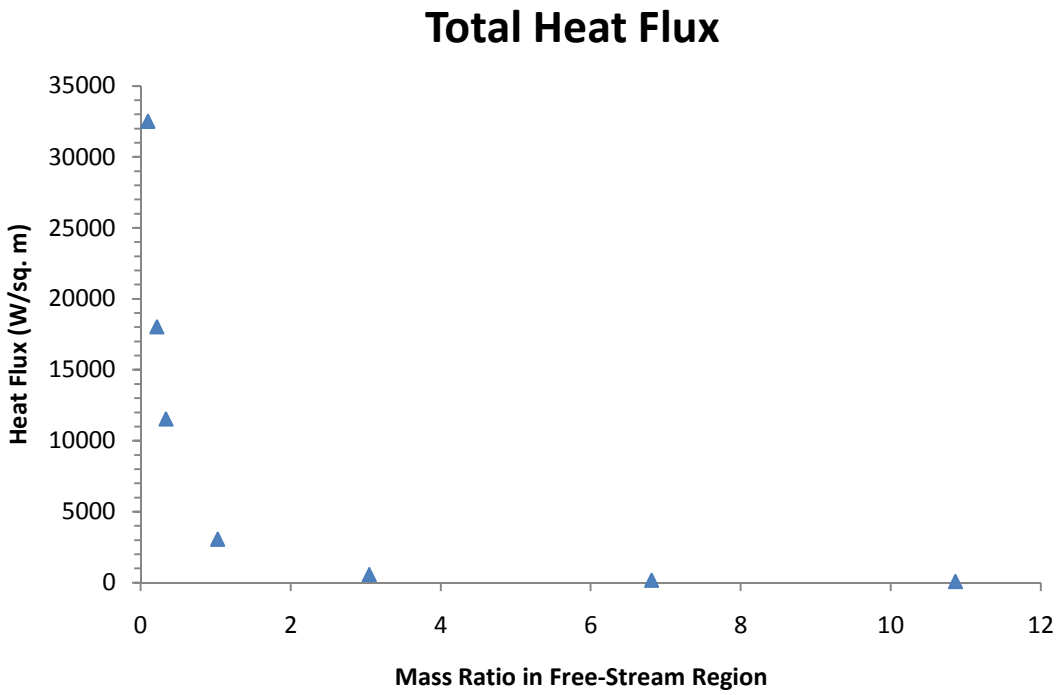

Figure 4 – Effect of mass ratio in the free-stream region on the heat flux at the interface

The influence of the presence of the noncondensable gas on condensation is highlighted by the above plots. As the mass ratio decreases, and thus the mass contribution of the air decreases, the heat transfer and condensation rates increase significantly. The inclusion of just a small amount of air causes a significant decrease in the amount of energy transferred. The energy release theoretically approaches infinity as the mass ratio approaches zero. The heat transfer through convection becomes smaller relative to the contribution of condensation when there is much more steam in the mixture.

Moreover, the results obtained for the cases shown in Table 1 are compared with previously-established models. The correlations proposed by Uchida and Tagami are not sufficient to account for temperature variation at the wall. If a wide range of free-stream temperatures were to be used for a constant wall temperature, the material phase enforcement would be broken. The results are plotted against values computed using the Peterson model. The reference point used for Equation 5 is the interface, as that is the location at which condensation is considered.

Figure 5 below shows the total heat transfer coefficient plotted against the gas-vapor log mean concentration ratio. This independent variable, which is introduced by Peterson, is used because it accounts for the conditions in both the free-stream and at the gas-liquid interface. Peterson's results are independent of the distance down the wall; they are also independent of a wall length, in the case of average computation. Although the Grashof number in the Nusselt and Sherwood numbers formulations is local, the effect of the change with distance is eventually removed when calculating the local heat transfer coefficient. This is due to the distance variable in the definition of the Nusselt and Sherwood numbers.

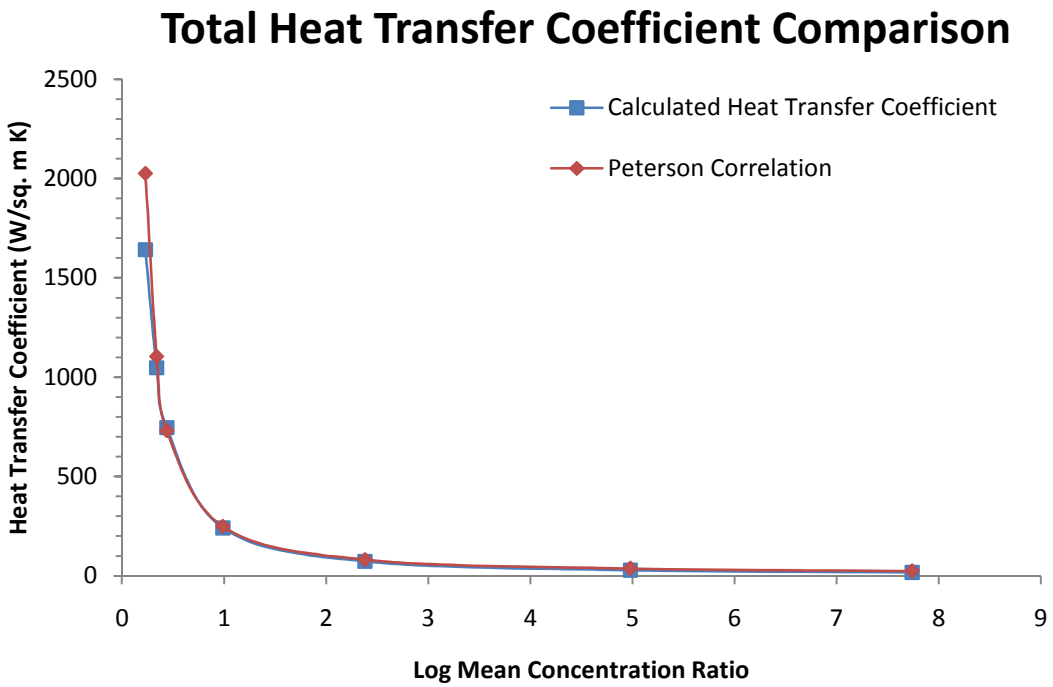

Figure 5 – Total heat transfer coefficient results compared with Peterson model

The plot shows that the calculated results under-predict the heat transfer coefficients at the local solution distance in a mixture where the air mass fraction is low in the free-stream region. That is important to state because of the distinct nature of the Peterson correlations compared to this model's results. The dependence on distance can be used to partially explain discrepancy in the plot shown. Depending on the distance at which the solution is determined, the heat transfer coefficients can be matched to those of Peterson. A local solution was deemed more beneficial because it can give a designer an idea of what the maximum value may be for a certain application. Local values can also be used to obtain a mean, so that process is not hindered by focusing on the local solutions. Another explanation can be attributed to the nature of this analysis; this analysis is based on numerical approximation procedures.

Moreover, the fact that the comparison shows deviation when there is very little air in the mixture is intriguing. The approximate profiles used in the analysis were obtained from natural convection problems in which the fluid was pure air. It can be hypothesized that that may have also had an effect on the results when there is little air in the mixture.

Previously, it was mentioned that the turbulent properties were very small relative to the molecular properties. To show the impact of the inclusion of the turbulence model proposed on the overall model, the results presented above are compared to results obtained by neglecting turbulent properties. Figure 6 illustrates this comparison.

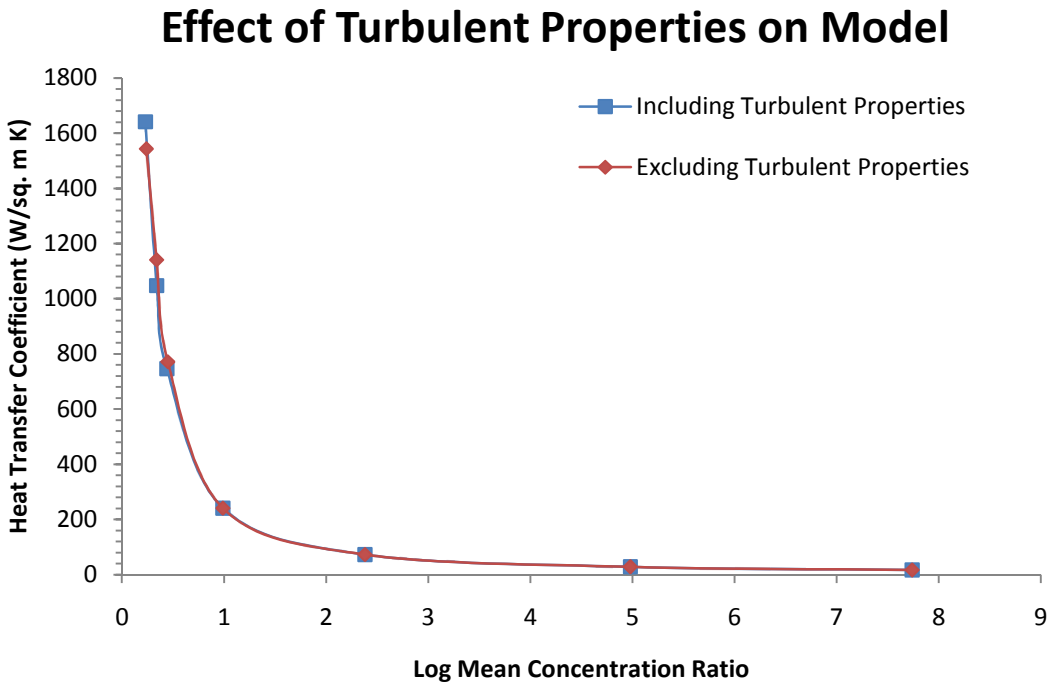

Figure 6 – The effect of turbulence properties on the model

At large air mass fraction quantities, the effect of turbulent flow properties is practically negligible. At low air presence, the effect becomes noticeable, but it is still not great. During the analysis procedure, the inclusion of turbulent properties does not only

affect the results due to their addition to the molecular properties; it also affects the convergence process on temperature. The turbulent viscosity, mass diffusion coefficient, and thermal conductivity parameters are in the energy balance equation.

To note the effect of the mass ratio in the free-stream region on the properties of the mixture throughout the boundary layer, the total density is plotted. The dimensional form of the values is plotted against the dimensionless distance, where unity represents the edge of the boundary layer. Figure 7 presents the total density for four cases that show a wide range of free-stream mass ratio values.

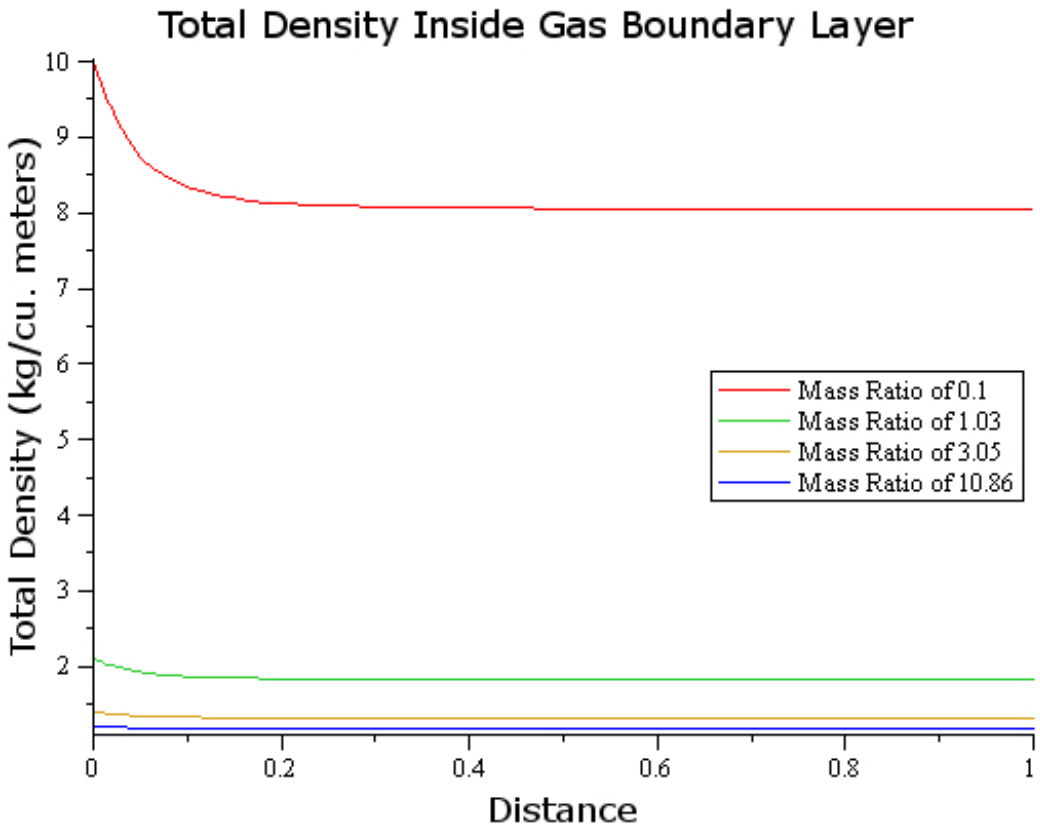

Figure 7– Density profiles for various free-stream mass ratio cases

The density does not vary significantly for cases where there is a great amount of air in the mixture, but at high pressure conditions, the density changes dramatically near the gas-liquid interface. This significant change is the reason the variation of density was not excluded in the model proposed.

CONCLUSION

The two main objectives of this analysis were accomplished. Approximate algebraic formulations were obtained to model this problem, and a program was written to automate the solution process. The algebraic approximations greatly simplify the solution method for this condensation natural convection process. Modeling a complex system of coupled non-linear partial differential equations using algebraic formulas is a significant move to simplify the design process. Local formulations are presented, but average values can be determined by integrating over the entire length of the wall.

To summarize, the results obtained suggest that for often times more realistic and larger temperature differences, condensation within the boundary layer must be considered. This is one limitation posed by the proposed model. The quality of saturation was enforced in many facets of the analysis process. The model outputs reasonable results for those cases where the vapor is saturated throughout the gas boundary layer. This is shown through the comparison made to a previously established model. Also, the partial pressure of the air in this analysis was maintained constant at one atmosphere outside the boundary layer; this is not necessarily a limitation, but the effects if its variation were not explored. The effect of the free-stream concentration of the air on condensation will be more or less significant depending on the change.

To further explore that point, the solutions also showed a reasonable relationship between the rate of heat transfer and the amount of air in the system. As the mass fraction of the air increased in relation to the mass of the vapor, the heat flux decreased. With the inclusion of just a small amount of air, the rate of decline is great, but the value eventually stabilizes as the amount of air in the free-stream region increases to large relative quantities. This relationship abides by the expectations mentioned in the onset.

FUTURE WORK

Turbulent flows are of most significance in design, as often times engineers are interested in the large velocity flow or large heat transfer rates. For future improvements to the current mathematical model, the vertical velocity at the interface should be set to the velocity of the liquid film there; this is in addition to imposing continuity of the shear stress between the two immiscible fluids. It would become similar to a Couette flow boundary condition with such modification.

In further pursuit of mathematical modeling, future work must consist of the inclusion of drop-wise condensation within the gas boundary layer. This addition is necessary to obtain results that can be used in solving problems with very large changes in temperature. Modifications would have to be made to the mass and momentum conservation laws to account for this, and an internal heat generation term would also be needed for the energy equation.

REFERENCES

[1] Amano, Ryoichi, and Bengt Suden. *Thermal Engineering in Power Systems*. Springer, 2008.

[2] Kim, Jong-Wong, Y. Lee, H. Ahn, and G. Park. *Condensation Heat Transfer Characteristic in the Presence of Noncondensable Gas on Natural Convection at High pressure*. Nuclear Engineering and Design 239. pp. 688-698 (2009).

[3] Bejan, Adrian. *Heat Transfer*. John Wiley & Sons, Inc., 1993.

[4] Eckert, E. R. G., and T. W. Jackson, *Analysis of Turbulent Free-convection Boundary Layer on Flat Plate*. NACA Report 1015 (1951).

[5] Warner, C. Y.. *An Experimental Investigation of Turbulent Natural Convection in Air at Low Pressure Along a Vertical Heated Flat Plate*. International Journal of Heat and Mass Transfer; Volume 11, pp. 397-406 (1967).

[6] Cheesewright, R., and E. Ierokipiotis, *Velocity Measurements in a Turbulent Natural Convection Boundary Layer*. Proceedings of the 7th International Heat Transfer Conference, Vol. 2, pp. 305-309 (1982).

[7] Squire, H. B.. *Modern Developments in Fluid Dynamics*. Oxford University Press, New York (1938).

[8] Mattingly, B. T., and N. E. Todreas. *MIT Advanced Containment Project: Review of Condensation Models and Computer Code Evaluation*. PhD Thesis. Massachusetts Institute of Technology (1997).

[9] Peterson, P. F., Schrock, V.E, Kageyama, T.. *Diffusion Layer Theory for Turbulent Vapor Condensation with Noncondensable Gases*. Journal of Heat Transfer; Volume 115, pp. 998–1003 (1993).

[10] Incropera, Frank, David Dewitt, Theodore Bergman, and Adrienne Lavine. *Fundamentals of Heat and Mass Transfer*. Sixth Edition. John Wiley & Sons, Inc. 2007.

[11] O'Connell, John, and J. M. Haile. *Thermodynamics: Fundamentals for Application*. Cambridge. 2005.

[12] Borggaard, Jeff. *Computational Methods for Optimal Design and Control*. Brikhauser. 1998.

[13] Jischa, Michael, and H. B. Rieke. *About the Prediction of Turbulent Prandtl and Schmidt Numbers from Modeled Transport Equations*. International Journal of Heat and Mass Transfer; Volume 22, pp. 1547-1555 (1979).

[14] Leach, James. *Thermal System Design*. North Carolina State University (1995).

[15] Cenjel, Yunus. *Heat Transfer: A Practical Approach*. Second Edition. McGraw-Hill. 2003.

APPENDICES

APPENDIX A

The temperature profile described by Equation 16 is compared to Warner's data and the profile used by Eckert.

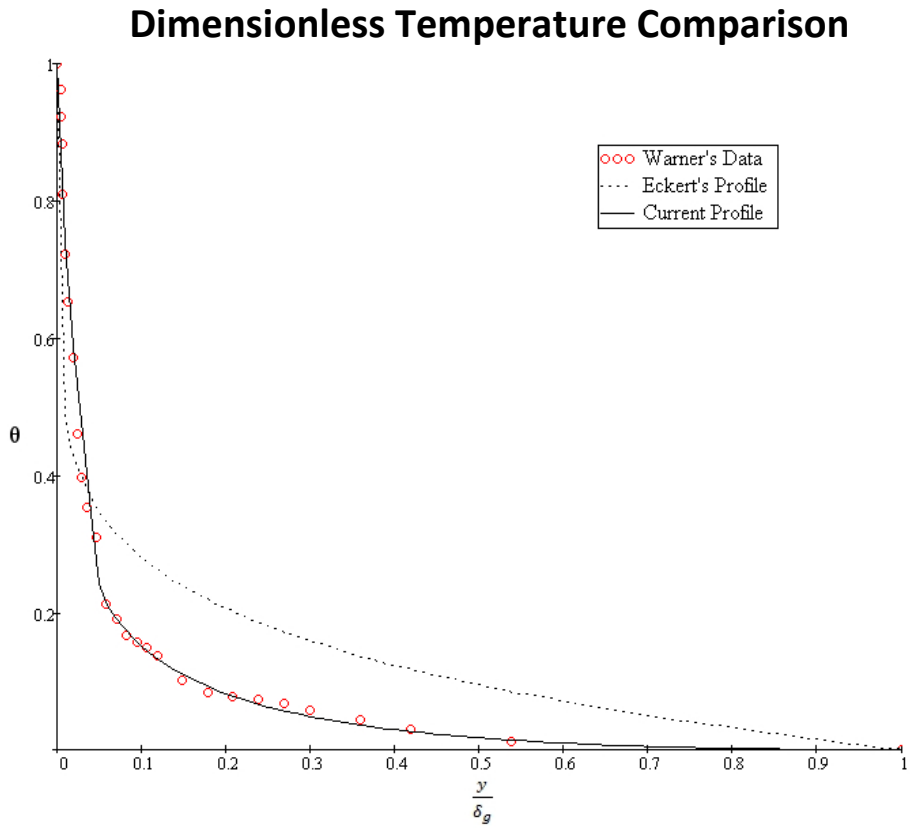

Figure A-1 – The temperature profile used is compared to Warner's data

The velocity profile used by Eckert and described by Equation 15 is compared to Cheesewright's data.

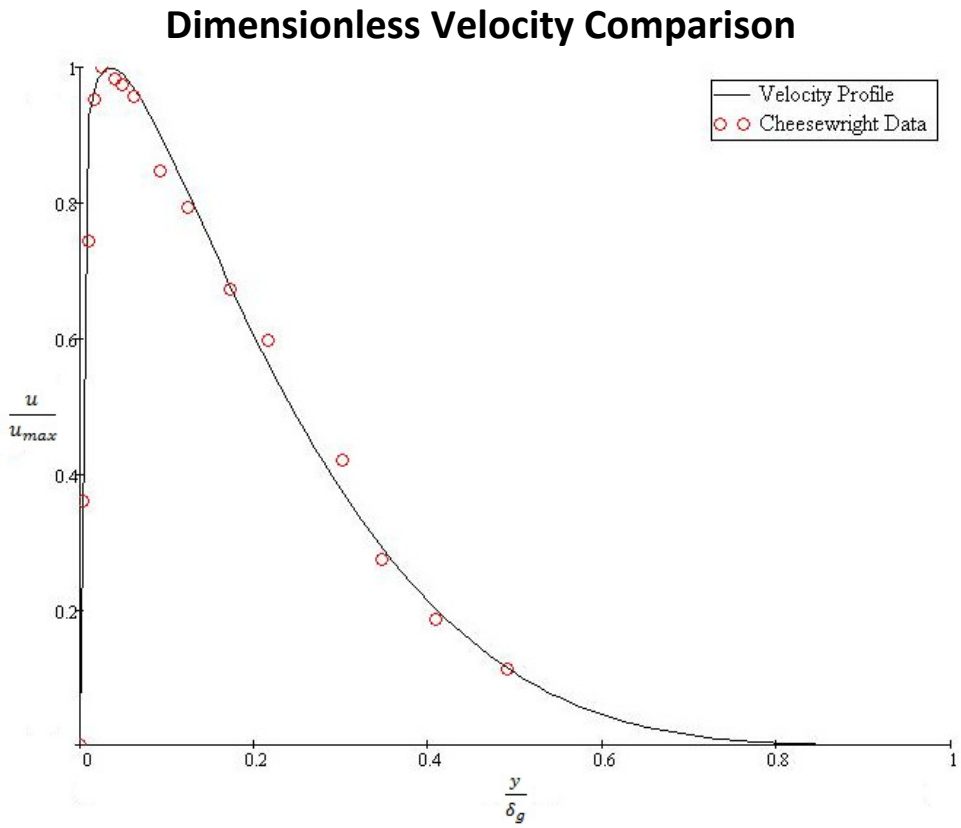

Figure A-2 – The velocity profile used is compared to Cheesewright's data

To show an example, the density profile described by Equation 17 is compared to tabulated data for a specific case of thermodynamic conditions. The free-stream and interface temperature values for the example below are 202°C and 49°C, respectively.

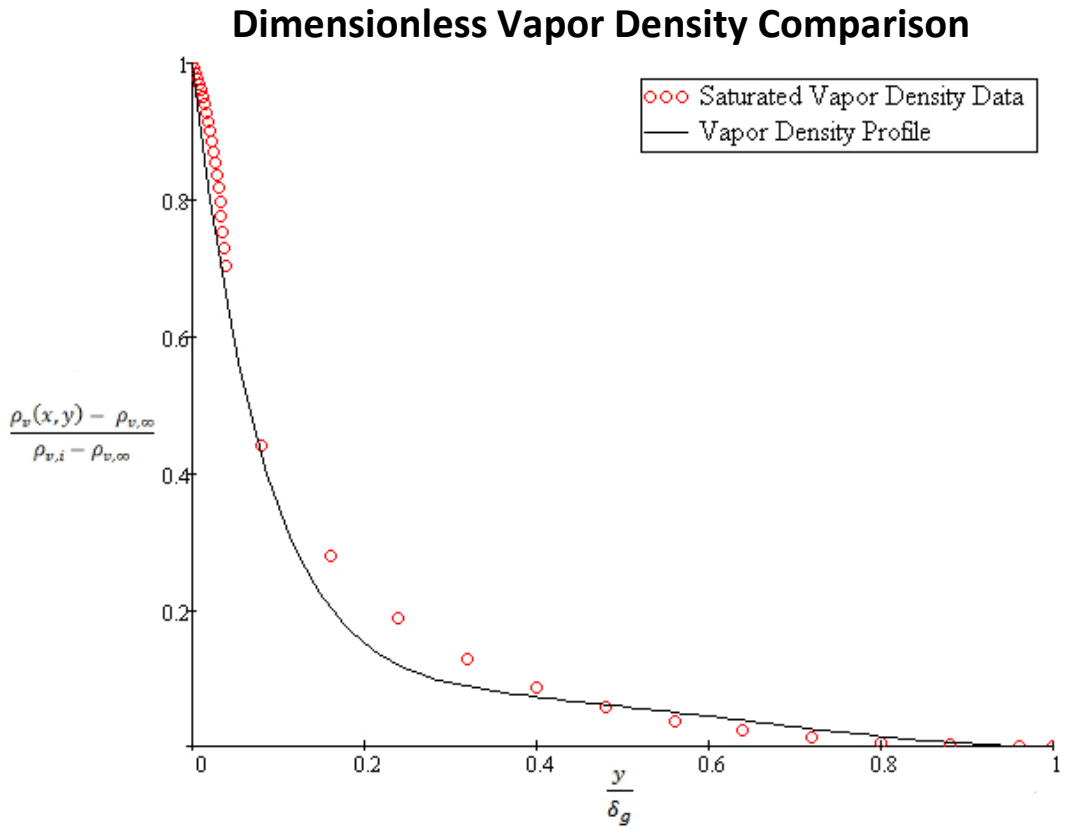

Figure A-3 – An example to show the vapor density profile

APPENDIX B

Determining the thermal conductivity of the binary mixture of air and vapor:

$$k = d_a k_a + d_v k_v \qquad \text{(B-1)}$$

Using Equation 41b,

$$b_{a,a} = 1$$

$$b_{v,v} = 1$$

$$b_{a,v} = 0.25\left(1 + \left[\frac{\mu_a}{\mu_v}\left(\frac{M_v}{M_a}\right)^{0.75}\frac{T + S_a}{T + S_v}\right]^{0.5}\right)^2 \frac{T + S_{a,v}}{T + S_a}$$

$$b_{v,a} = 0.25\left(1 + \left[\frac{\mu_v}{\mu_a}\left(\frac{M_a}{M_v}\right)^{0.75}\frac{T + S_v}{T + S_a}\right]^{0.5}\right)^2 \frac{T + S_{v,a}}{T + S_v}$$

$$S_v = 1.5T_{boiling}$$

$$S_a = 110\ K$$

$$S_{a,v} = S_{v,a} = (S_a S_v)^{0.5}$$

Using the above results, the coefficients in Equation B-1 can be calculated.

$$d_a = \frac{X_a}{b_{a,a}X_a + b_{a,v}X_v}$$

$$d_v = \frac{X_v}{b_{v,v}X_v + b_{v,a}X_a}$$

APPENDIX C

Specific sections of the code used to solve this problem are presented here. The lines associated with the interface temperature solution are shown below.

```
C   Determining the Film Heat Transfer Coefficient
      cpf=4010.0
      hfgp=(-hgf(ti))+.68*cpf*(ti-tw)
      hf=4.0*mufilm(ti)*(ti-tw)*xsol
      hf=((hf/(g*hfgp*((kfilm(ti))**3.0)*(rhofilm(ti)**2.0)))**(-0.25))
C   Determining the Heat Transfer Coefficient Attributed to Pure Convection
      hconv=0.0359*(rhovi*dcp+cpa*ptot/(ra*ti))*((nui+nuit)**(0.25))
      hconv=hconv*(deltag(xsol)**(-0.25))*(umax(xsol)**(0.75))
C   Determining the Heat Transfer Coefficient Attributed to Condensation
      ccond=davieff*ptot*pviprime/(rv*(ptot-pvi)*(ki+kit))
      hcond=hconv*ccond*(-hgf(ti)+.68*cpv*(-dt))
C   Solving for the Interface Temperature
C   Tie is a placeholder name given to Ti through this iteration.
      tie=(hf*tw+(hcond+hconv)*tinf)/(hf+hconv+hcond)
      difft=abs(tie-ti)
      ti=tie
      if(difft.GT.0.0001) go to 40
```

The following are the lines showing an example of how the integration procedure was performed for one term in the program. Since two sub-domains are used for the temperature profile, the limits of integration were constantly overwritten throughout the program to update the discretization of the curves.

```
C   3rd Integral in Convection Side of Energy Equation
      a=0.0
      b=0.059
      h=b-a
      dy=h/n
      sum=19*fthree(a)+19*fthree(b)
      w=75
      do 318 i=1,n-4,5
      y=a+i*dy
      sum=sum+w*fthree(y)
318   continue
      do 328 i=4,n-1,5
      y=a+i*dy
      sum=sum+w*fthree(y)
328   continue
      w=50
      do 338 i=2,n-3,5
      y=a+i*dy
      sum=sum+w*fthree(y)
338   continue
      do 348 i=3,n-2,5
      y=a+i*dy
      sum=sum+w*fthree(y)
348   continue
      w=38
      do 358 i=5,n-5,5
      y=a+i*dy
      sum=sum+w*fthree(y)
358   continue
      fthreeint=sum*5*dy/288
```

The following are the lines associated with the convergence of the turbulent viscosity. It is mainly comprised of the Newton-Raphson method. "fnut" represents the semi-empirical one-equation turbulence model introduced in the Turbulence Modeling section. There is a loop highlighted by line 401 where the zero convergence is performed. Once the zero is found, the comparison is made between an initial value and the updated value.

```
      cmu=0.09**(0.25)
      cl=0.09
      cnut=(0.00632)*cmu*cl*ptot*pviprime*(tinf-ti)*rhocpi
      cnut=cnut*((deltag(xsol)*umax(xsol))**(0.75))
      cnut=(cnut)/(rhoi)
      cnut=(cnut)/(rv)
      cnut=(cnut)/(ptot-pvi)
      stp=0.00000001
      nut=nuit
401   nut=nut-(fnut(nut)/fnutprime(nut))
      dnut=fnut(nut)/fnutprime(nut)
      if(dnut.GT.0.001) go to 401
      if(dnut.LT.-0.001) go to 401
      diffnu=abs(nut-nuit)
      nuit=nut
      if(diffnu.GT.0.00000001) go to 41
```